



A nitrogen stress-inducible small RNA regulates CO₂ fixation in *Nostoc*

Manuel Brenes-Álvarez ¹, Elvira Olmedo-Verd ¹, Agustín Vioque ¹ and Alicia M. Muro-Pastor ^{1,*†}

¹ Instituto de Bioquímica Vegetal y Fotosíntesis, Consejo Superior de Investigaciones Científicas and Universidad de Sevilla, Seville E-41092, Spain

*Author for communication: alicia@ibvf.csic.es

†Senior author.

These authors contributed equally (M.B.A., E.O.V.)

M.B.A., E.O.V., A.V., and A.M.M.P. designed and performed the experiments and analyzed the data; A.V. and A.M.M.P. supervised the work and wrote the article with contributions of M.B.A. and E.O.V. A.M.M.P. agrees to serve as the author responsible for contact and ensures communication.

The authors responsible for distribution of material integral to the findings presented in this article in accordance with the policy described in the Instructions for Authors (<https://academic.oup.com/plphys/pages/general-instructions>) is: Alicia M. Muro-Pastor (alicia@ibvf.csic.es)

Abstract

In the absence of fixed nitrogen, some filamentous cyanobacteria differentiate heterocysts, specialized cells devoted to fixing atmospheric nitrogen (N₂). This differentiation process is controlled by the global nitrogen regulator NtcA and involves extensive metabolic reprogramming, including shutdown of photosynthetic CO₂ fixation in heterocysts, to provide a micro-aerobic environment suitable for N₂ fixation. Small regulatory RNAs (sRNAs) are major post-transcriptional regulators of gene expression in bacteria. In cyanobacteria, responding to nitrogen deficiency involves transcribing several nitrogen-regulated sRNAs. Here, we describe the participation of nitrogen stress-inducible RNA 4 (NsiR4) in post-transcriptionally regulating the expression of two genes involved in CO₂ fixation via the Calvin cycle: *glpX*, which encodes bifunctional sedoheptulose-1,7-bisphosphatase/fructose-1,6-bisphosphatase (SBPase), and *pgk*, which encodes phosphoglycerate kinase (PGK). Using a heterologous reporter assay in *Escherichia coli*, we show that NsiR4 interacts with the 5'-untranslated region (5'-UTR) of *glpX* and *pgk* mRNAs. Overexpressing NsiR4 in *Nostoc* sp. PCC 7120 resulted in a reduced amount of SBPase protein and reduced PGK activity, as well as reduced levels of both *glpX* and *pgk* mRNAs, further supporting that NsiR4 negatively regulates these two enzymes. In addition, using a *gfp* fusion to the *nsiR4* promoter, we show stronger expression of NsiR4 in heterocysts than in vegetative cells, which could contribute to the heterocyst-specific shutdown of Calvin cycle flux. Post-transcriptional regulation of two Calvin cycle enzymes by NsiR4, a nitrogen-regulated sRNA, represents an additional link between nitrogen control and CO₂ assimilation.

Introduction

In response to nitrogen deficiency, some filamentous cyanobacteria are able to differentiate a specialized cell type devoted to fixation of atmospheric nitrogen, the heterocyst (Muro-Pastor and Hess, 2012). Differentiation of functional heterocysts, which takes about 24 h to complete under laboratory conditions, involves a precise gene expression program in which many genes are distinctly regulated in cells

undergoing transformation into heterocysts (Brenes-Álvarez et al., 2019). This program is ultimately under the control of the global nitrogen regulator NtcA (Herrero et al., 2004) but also involves HetR, the master regulator of cellular differentiation (Buikema and Haselkorn, 1991) that is required for expression of the heterocyst-specific transcriptome (Brenes-Álvarez et al., 2019). In N₂-fixing filaments, composed of vegetative cells and heterocysts, metabolic division of labor is

established so that photosynthesis and N_2 fixation are spatially separated in the two different cell types that cooperate to achieve growth of the filament as a whole. Whereas the vegetative cells maintain photosynthesis and CO_2 fixation, providing reduced carbon to heterocysts, the heterocysts provide fixed nitrogen through nitrogenase activity (Flores and Herrero, 2010; Herrero et al., 2016). One major aspect of the metabolic reprogramming of vegetative cells undergoing differentiation as heterocysts involves shutdown of oxygenic photosynthesis, which is not compatible with the activity of the O_2 -inactivated enzyme nitrogenase. Early studies showing movement of reduced carbon compounds from vegetative cells into heterocysts suggested that there was no CO_2 fixation in heterocysts (Fay and Walsby, 1966; Wolk, 1968), consistent with the absence in those cells of key enzymes of the Calvin cycle, such as ribulose-bisphosphate carboxylase/oxygenase (Rubisco) or phosphoribulokinase (PRK; Codd and Stewart, 1977; Codd et al., 1980; Cossar et al., 1985; Elhai and Wolk, 1990). In agreement with those observations, a quantitative proteomic study in *Nostoc punctiforme* showed that proteins involved in the carbon concentrating mechanism and enzymes involved in CO_2 fixation were present in reduced amounts in the heterocysts versus the vegetative cells (Sandh et al., 2014).

Carbon and nitrogen metabolisms are tightly coupled in cyanobacteria, with regulatory circuits depending on the balance between these two elements (Zhang et al., 2018; Herrero and Flores, 2019; Forchhammer and Selim, 2020). NtcA, the main transcriptional regulator of nitrogen assimilation, is modulated by the level of 2-oxoglutarate, an indicator of the C/N balance that integrates the flow of CO_2 assimilation through the Calvin–Benson cycle and ammonium (NH_4^+) assimilation through the GS/GOGAT cycle (Vázquez-Bermúdez et al., 2002). Central to C/N homeostasis in cyanobacteria is the nitrogen-regulated expression of elements involved in carbon assimilation, such as the recently described carbon flow regulator CfrA/PirC whose transcription is directly activated by NtcA (Muro-Pastor et al., 2020; Orthwein et al., 2021). In addition to transcriptional regulation, post-transcriptional regulatory mechanisms might also play a relevant role in achieving properly balanced assimilation of carbon and nitrogen (Muro-Pastor and Hess, 2020).

Post-transcriptional regulation by noncoding RNAs (small regulatory RNAs [sRNAs] and antisense RNAs) is emerging as an additional level of control of different processes in bacteria. Noncoding RNAs whose transcription is regulated in response to certain environmental changes are candidates for having a role in the adaptation to those changes. For instance, a major transcription factor in cyanobacteria, RpaB, which regulates adaptation to fluctuating light conditions (Wilde and Hihara, 2016), regulates expression of PsrR1 (Kadowaki et al., 2016), an sRNA that controls photosynthetic functions (Georg et al., 2014). Several nitrogen-regulated sRNAs have been identified both in unicellular and heterocystous cyanobacterial strains. In the case of *Nostoc*

sp. PCC 7120 (also known as *Anabaena* sp. PCC 7120, hereafter *Nostoc*), sRNAs have been described with NtcA-regulated expression, such as NsiR3, NsiR4, or NsrR1 (Klähn et al., 2015; Álvarez-Escribano et al., 2018, 2021) or with HetR regulated, heterocyst-specific expression, such as NsiR1 (Ionescu et al., 2010).

NsiR4 is a small RNA widely distributed among cyanobacterial strains. Two versions, which differ in the presence of a 5'-extension capable of forming a short hairpin, have been identified. Long 5'-extended forms are found in unicellular strains, such as the nondiazotrophic strain *Synechocystis* sp. PCC 6803 (hereafter *Synechocystis*), whereas shorter versions are present in filamentous strains, including those capable of fixing N_2 via differentiation of heterocysts, such as *Nostoc*. In all cases, the corresponding promoters contain binding sites for NtcA, and NtcA has been shown to activate expression of NsiR4 in response to nitrogen deprivation in both *Synechocystis* and *Nostoc* (Klähn et al., 2015). In *Synechocystis*, NsiR4 post-transcriptionally regulates accumulation of IF7, one of the inactivating factors that modulate the activity of glutamine synthetase, a key enzyme involved in nitrogen assimilation, therefore participating in a regulatory feed-forward loop operated by NtcA (Klähn et al., 2015).

In this work, we provide evidence showing that accumulation of bifunctional sedoheptulose-1,7-bisphosphatase/fructose-1,6-bisphosphatase (SBPase) and phosphoglycerate kinase (PGK) is subjected to post-transcriptional regulation involving NsiR4. We also show that expression of NsiR4 is stronger in heterocysts than in vegetative cells, and could therefore contribute to the differential regulation of these two enzymes of the Calvin cycle specifically in heterocysts. Ultimately, regulation of CO_2 fixation by an NtcA-regulated sRNA represents a link between nitrogen availability and carbon assimilation.

Results

NsiR4 is conserved in heterocystous cyanobacteria and accumulates differentially in heterocysts

Sequences encoding NsiR4 are strongly conserved among heterocystous cyanobacteria and would produce an sRNA with a single-stranded stretch followed by a terminator stem loop (Supplemental Figure S1). In *Nostoc*, the sequence encoding the NsiR4 homolog is located tail to tail with that of the coding region of *alr3725* (Figure 1A) and is transcribed from a transcriptional start site (TSS) located at position 4499325r (Mitschke et al., 2011), downstream of a NtcA-regulated promoter (Figure 1B). Northern blot hybridization shows that expression of NsiR4 is already observed 3–6 h after nitrogen removal, both in the wild-type (WT) and in a *hetR* mutant strain unable to differentiate heterocysts (Figure 1, C and D), suggesting transcription of NsiR4 would be induced in all cells of the filaments upon nitrogen stress. In order to analyze expression of NsiR4 in specific cells of N_2 -fixing filaments, we constructed a fusion between the

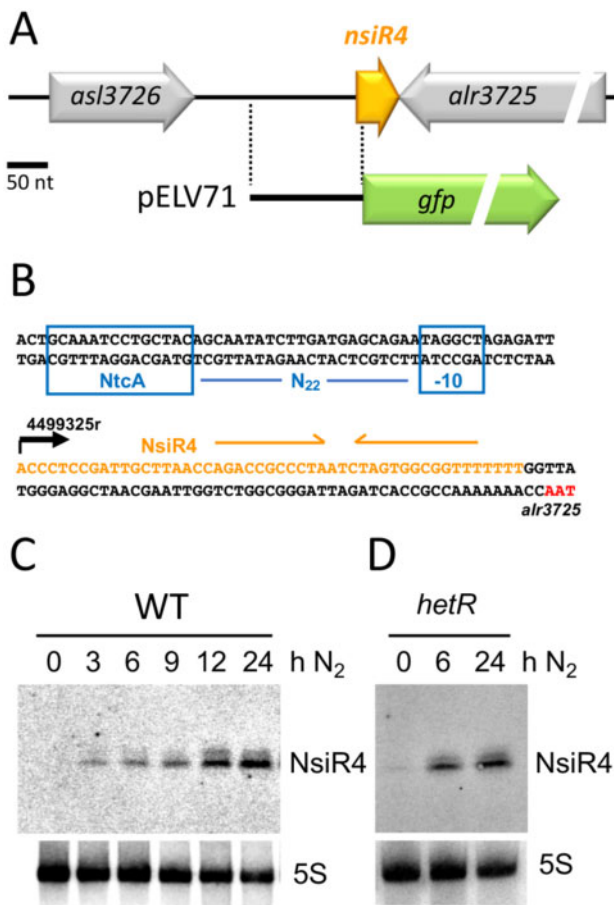


Figure 1 NsiR4 in *Nostoc*. A, Schematic representation of the region encoding NsiR4. The flanking annotated open reading frames are indicated (gray arrows), together with NsiR4 (orange arrow) and the promoter region cloned upstream of the *gfp* gene (green arrow) in promoter-probe plasmid pELV71. B, Sequence of the promoter and coding region of NsiR4. The sequence encoding NsiR4 (in orange), the stop codon of *alr3725* (in red), as well as the NtcA-binding box, the -10 box, the spacing between both boxes (22 nt), and the TSS (black arrow) are indicated. Sequences producing a stem-loop terminator are indicated with orange arrows. C and D, Nitrogen-responsive expression of NsiR4 in *Nostoc* WT (C) and *hetR* mutant strain 216 (D). Expression was analyzed by Northern blot in cells grown in the presence of NH_4^+ and transferred to a medium containing no source of combined nitrogen for the number of hours indicated. The upper panels show hybridization to a probe for NsiR4. The lower panels show hybridization to a probe for 5S RNA used as loading and transfer control. Samples contained 10 μg of total RNA.

promoter of NsiR4 and the *gfp* gene (see the scheme of plasmid pELV71 in Figure 1A). Filaments bearing plasmid pELV71 showed very low green fluorescence in the presence of NH_4^+ while filaments growing on nitrogen-free medium showed increased green fluorescence in vegetative cells, with peaks of strong fluorescence associated with heterocysts (Figure 2A). Fluorescence in individual vegetative cells from filaments growing in the presence of NH_4^+ or in the absence of combined nitrogen was quantified as indicated in the scheme (Figure 2B), showing ~ 2.5 -fold induction of the

nsiR4 promoter in vegetative cells of N_2 -fixing filaments compared with vegetative cells of filaments growing in the presence of NH_4^+ .

CopraRNA predicts *glpX* and *pgk* mRNAs as possible targets of NsiR4 in *Nostoc*

Prediction of mRNAs that might be post-transcriptionally regulated by NsiR4 was carried out using the CopraRNA algorithm, which takes into account comparative phylogenetic information (Wright et al., 2013, 2014). The top 10 predicted interactions using the genomes of 9 heterocystous cyanobacteria, including *Nostoc*, are shown in Table 1. Because functional enrichment among the possible targets of sRNA regulation can be taken as a further indication of the validity of predictions, two of the best-predicted targets caught our attention, since they correspond to mRNAs encoding two enzymes involved in CO_2 assimilation by the Calvin–Benson cycle, namely SBPase, encoded by gene *glpX* (*alr1041*), and PGK, encoded by gene *pgk* (*all4131*). In addition, according to transcriptomic analysis, accumulation of *glpX* and *pgk* mRNAs is lower under nitrogen deficiency (Brenes-Álvarez et al., 2019; see also Supplemental Figure S2). This observation would be consistent with possible negative effects on mRNA stability caused by interaction with a nitrogen stress-inducible sRNA such as NsiR4.

The predicted interactions between NsiR4 and the 5'-UTR of the mRNAs of *glpX* and *pgk* would take place immediately upstream of the translational start codon (GUG in both cases), overlapping the Shine–Dalgarno (SD) sequence (Figure 3), and therefore would affect translation of the mRNAs. In accordance with CopraRNA results, such interactions would be phylogenetically conserved in many heterocystous cyanobacteria (Supplemental Figure S3).

NsiR4 interacts with *glpX* and *pgk* mRNAs

We have validated the predicted interactions between NsiR4 and the mRNAs of *glpX* and *pgk* using a heterologous reporter assay (Corcoran et al., 2012) in which two plasmids, one producing constitutive expression of a predicted target mRNA and the other of the sRNA under study, are combined in *Escherichia coli* cells. One of the plasmids encodes the 5'-UTR of the predicted *glpX* or *pgk* target (plus the first 60 nucleotides [nt] of the coding sequence) translationally fused to the gene for *superfolder* green fluorescent protein (sfGFP), whereas the other plasmid encodes NsiR4 or an unrelated RNA used as a control. Cells bearing the fusion of either *glpX* or *pgk* to *sfGFP* showed fluorescence, indicating that both translation initiation regions were functional in *E. coli*, although to different extents (Figure 3, A–B). In fact, whereas in the case of *glpX* the GUG start codon had to be replaced by AUG to facilitate translation, such a change was not necessary in the case of *pgk*, which produced higher levels of fluorescence even with the native GUG start codon. In the case of both *glpX* (Figure 3A) and *pgk* (Figure 3B), the fluorescence in *E. coli* cells encoding the corresponding sfGFP fusion significantly decreased when NsiR4 was co-expressed, in comparison with cells expressing the control

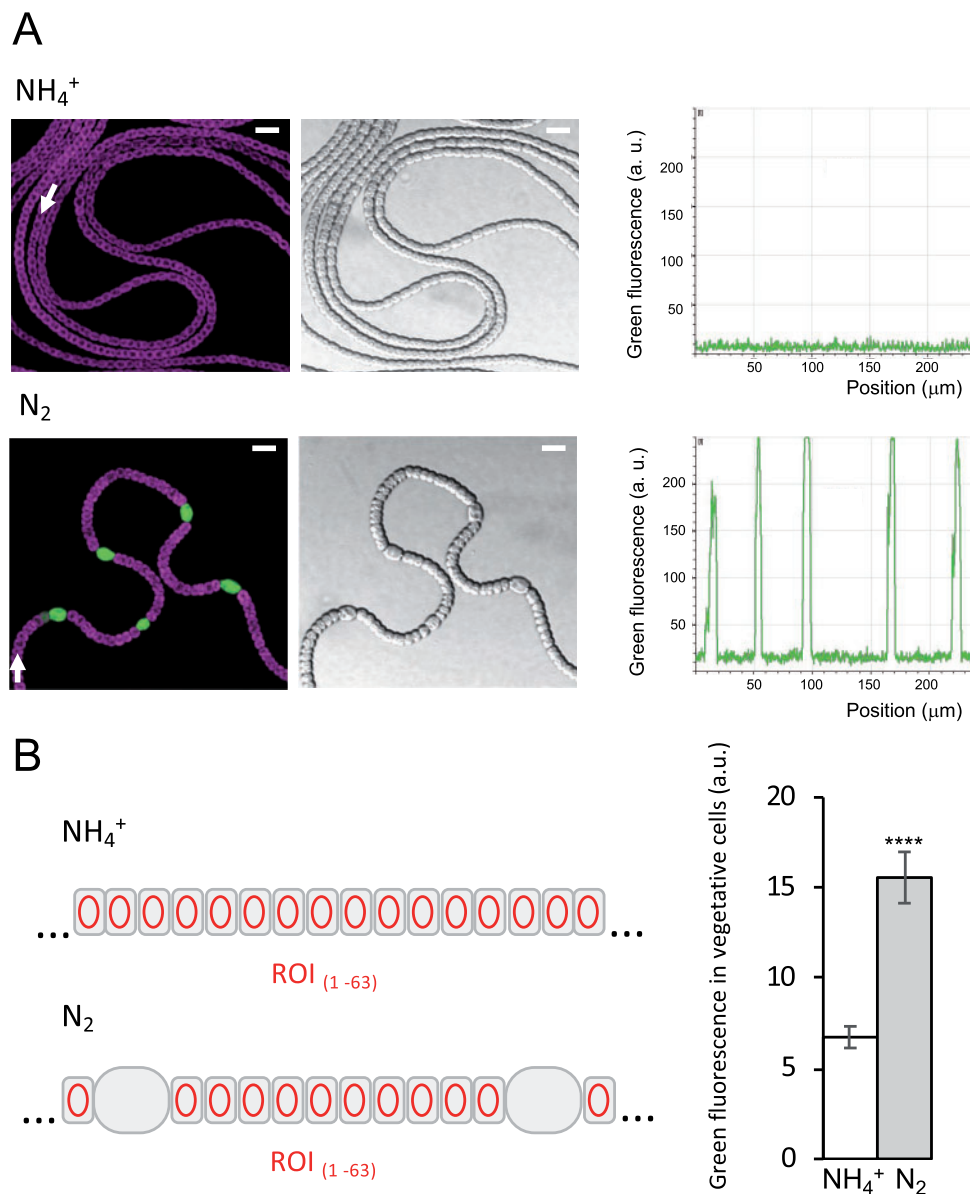


Figure 2 Expression of $P_{\text{NsiR4}}\text{-gfp}$. A, Confocal fluorescence images of filaments bearing plasmid pELV71 growing on top of medium containing ammonium (NH_4^+) or lacking any source of combined nitrogen (N_2) are shown with merged green (GFP fluorescence) and red (autofluorescence, shown in magenta) channels. Quantification of the signal for the green channel along the filaments indicated with white arrows is shown on the right. All images were acquired with the same sensitivity settings for the green channel so that intensities can be compared. Scale bars, 10 μm . B, Quantification of GFP fluorescence in vegetative cells of the filaments indicated with white arrows in (A). Sixty three regions of interest corresponding to vegetative cells were quantified for each condition (red ovals), as indicated in the scheme on the left. Data are presented on the right as the mean and standard deviation of the fluorescence. T test **** $P < 0.0001$.

Table 1 List of predicted interaction partners for NsiR4 based on the CopraRNA algorithm

Rank	P-value	Locus Tag	Gene	Annotation
1	1,65E-15	pcc7120delta_rs22335 (<i>all4121</i>)	<i>petH</i>	Ferredoxin-NADP(+) reductase
2	1,74E-10	pcc7120delta_rs22380 (<i>all4131</i>)	<i>pgk</i>	Phosphoglycerate kinase
3	1,68E-09	pcc7120delta_rs07060 (<i>alr1041</i>)	<i>glpX</i>	Fructose-1,6-bisphosphatase
4	5,55E-08	pcc7120delta_rs04675 (<i>alr0549</i>)	NA	Four helix bundle protein
5	4,36E-06	pcc7120delta_rs04815 (<i>all0578</i>)	<i>dnaB</i>	Intein-containing replicative DNA helicase
6	6,05E-06	pcc7120delta_rs05000 (<i>alr0617</i>)	<i>cpcS</i>	Phycocyanobilin lyase
7	8,24E-06	pcc7120delta_rs04560	NA	Hypothetical protein
8	2,23E-05	pcc7120delta_rs05130 (<i>alr0643</i>)	NA	MotA/TolQ/ExbB proton channel family protein
9	2,49E-05	pcc7120delta_rs21105 (<i>all3880</i>)	<i>cphB</i>	Cyanophycinase
10	2,73E-05	pcc7120delta_rs11495 (<i>all1943</i>)	NA	Hypothetical protein

NsiR4 sequences from the following strains were used: *Nostoc* sp. PCC 7120, *T. variabilis* ATCC 29413, *Calothrix* sp. PCC 6303, *C. stagnale* PCC 7417, *N. azollae* 0708, *N. punctiforme* PCC 73102, *Nostoc* sp. PCC 7524, *Rivularia* sp. PCC 7116, and *Nostoc* sp. PCC 7107. NA, not available. Genes studied in this work are indicated in bold.

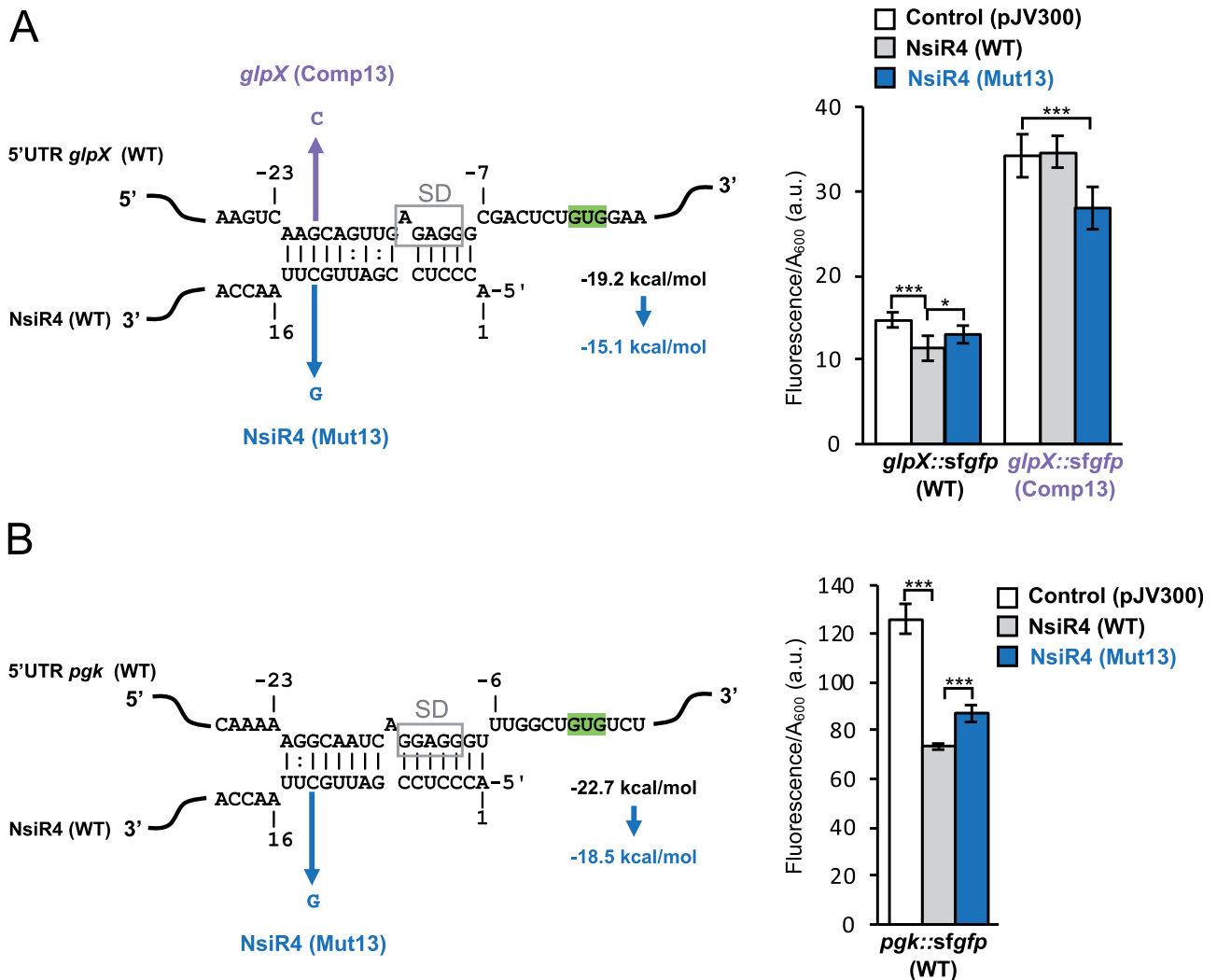


Figure 3 Verification of NsiR4 interaction with the 5'-UTR of *glpX* and *pgk* using an in vivo reporter system in *E. coli*. **A**, Left, predicted interaction between NsiR4 and the 5'-UTR of *glpX* according to IntaRNA (Mann et al., 2017). Nucleotides in the 5'-UTR are numbered with respect to the start of the coding sequence (shaded). The mutation introduced in NsiR4 at position 13 (C to G, Mut13) and the corresponding compensatory mutation in *glpX* 5'-UTR at position -20 (G to C, Comp13) are indicated in blue and purple, respectively. Hybridization energies of the interaction between the *glpX* mRNA and the WT (black) or mutated (blue) versions of NsiR4 are indicated. Right, fluorescence measurements of *E. coli* DH5 α cultures bearing combinations of plasmids expressing different versions of NsiR4 (WT or Mut13) and *glpX::sfgfp* fusions (WT or Comp13). Plasmid pJV300 was used as control. **B**, Left, predicted interaction between NsiR4 and the 5'-UTR of *pgk* according to IntaRNA (Mann et al., 2017). Nucleotides in the 5'-UTR are numbered with respect to the start of the coding sequence (shaded). The mutation introduced in NsiR4 at position 13 (C to G, Mut13) is indicated in blue. Hybridization energies of the interaction between the *pgk* mRNA and the WT (black) or mutated (blue) versions of NsiR4 are indicated. Right, fluorescence measurements of *E. coli* DH5 α cultures bearing combinations of plasmids expressing different versions of NsiR4 (WT or Mut13) and the *pgk::sfgfp* fusion. Plasmid pJV300 was used as control. **A** and **B**, Putative SD sequences are boxed. The data are presented as the mean \pm standard deviation of the results from eight independent colonies after subtraction of fluorescence in cells bearing plasmid pXG0. Fluorescence is normalized to the A_{600} of each culture. *T* test ****P* < 0.001; **P* < 0.05.

RNA, indicating that the interaction of NsiR4 with either the *glpX* or the *pgk* mRNAs negatively affected their translation.

To verify that the interactions took place at the predicted sites, a point mutation that would destabilize interaction with both the *glpX* and *pgk* mRNAs was introduced into NsiR4 (nt 13, C to G, Mut13). The corresponding hybridization energies to the WT and the mutated version of NsiR4 are indicated (Figure 3A and B). Mutation of NsiR4 diminished the interaction with both mRNAs, as indicated by a weaker reduction of fluorescence compared with cells

expressing native NsiR4. We additionally constructed a mutated version of the mRNA of *glpX* containing a compensatory change (nt -20, G to C, Comp13) that would restore interaction with the Mut13 version of NsiR4. In this case, the fluorescence of cells bearing the compensatory change in the 5'-UTR of *glpX* and expressing the Mut13 version of NsiR4 was reduced with respect to that of cells bearing NsiR4, indicating interaction between NsiR4 (Mut13) and *glpX* (Comp 13). The absolute fluorescence values of cells bearing the compensated version of *glpX* were in all cases

higher than those of the native version, presumably due to better efficiency in the translation of the compensated version versus the WT version. A similar compensatory mutation could not be analyzed in the case of the *pgk* mRNA because the fluorescence of the strain bearing the modified version of the mRNA was too low for accurate measurement.

glpX and *pgk* are post-transcriptionally regulated by NsiR4 in *Nostoc*

In order to analyze the effects of NsiR4 in *Nostoc*, we prepared strains with altered levels of NsiR4. In the overexpressor strains (OE_NsiR4), constitutive high levels of NsiR4 were transcribed from the strong *trc* promoter to the T1 terminator of *rrnB* of *E. coli* (Figure 4A). Because of the proximity of *nsiR4* with the gene located downstream (Figure 1), and in order to deplete NsiR4 while preserving the structure of the region, we took an approach based on the overexpression of an antisense sequence (complementary to NsiR4), which would act as a sponge to neutralize NsiR4 (OE_as_NsiR4). This approach has been successfully used to deplete other sRNAs in *Nostoc*, such as Yfr1, which is involved in cell wall homeostasis (Brenes-Álvarez et al., 2020b) or the nitrogen-stress-inducible NsiR1, which modulates heterocyst differentiation (Brenes-Álvarez et al., 2020a). We verified the accumulation of NsiR4 in *Nostoc* strains bearing the above-described constructs by Northern blot. In the overexpressor strains, NsiR4 molecules transcribed from the *trc* promoter bear a 6-nt tag so that they can be distinguished from native endogenous NsiR4 molecules based on their lengths. Expression of NsiR4 from the *trc* promoter clearly exceeded endogenous NsiR4 expression, whereas transcription of the sequence antisense to NsiR4 led to complete depletion of NsiR4 (Figure 4B). Both OE_NsiR4 and OE_as_NsiR4 strains could grow on agar plates, similarly to the OE_C control strain, in the presence of combined nitrogen, however, OE_NsiR4, unlike OE_as_NsiR4 or the control strain, could not grow under N₂-fixing conditions (Supplemental Figure S4).

We then analyzed the amount of SBPase and PGK in the strains with altered levels of NsiR4. Using antibodies against *Synechocystis* SBPase, we detected reduced amounts of SBPase protein in the strain overexpressing NsiR4 (OE_NsiR4), whereas a slightly increased amount of protein was observed in the strain depleted of NsiR4 (OE_as_NsiR4; Figure 4C). Similarly, reduced PGK activity was present in crude extracts of the strain overexpressing NsiR4, while higher PGK activity was found in crude extracts of the strain depleted of NsiR4 (OE_as_NsiR4; Figure 4D).

We also tested the accumulation of the mRNAs of *glpX* and *pgk* in the OE_C (control), OE_NsiR4 and the OE_as_NsiR4 strains. The accumulation of both mRNAs was significantly diminished in the strain overexpressing NsiR4 (OE_NsiR4) with respect to the control strain (Figure 4, E and F), and there was also a slightly increased accumulation of both mRNAs in the OE_as_NsiR4, which was

depleted of NsiR4. Taken together, these results indicated that NsiR4 negatively affects the accumulation of *glpX* and *pgk* mRNAs in *Nostoc*. This is the expected result if inhibition of their translation by NsiR4 results in destabilization of the mRNAs.

Discussion

Cyanobacteria have evolved sophisticated regulatory networks in order to keep a proper carbon/nitrogen balance (Forchhammer and Selim, 2020). In addition to transcriptional regulation, mechanisms involving post-transcriptional regulation by noncoding RNAs appear to play a role in the coordination of carbon and nitrogen assimilation in these photosynthetic bacteria (Muro-Pastor and Hess, 2020). Here we describe the participation of NsiR4, a NtcA-regulated sRNA, in the post-transcriptional regulation of *glpX* and *pgk*. The conserved binding site of NsiR4 on the translation initiation region of these two mRNAs overlaps the predicted ribosome binding site (Figure 3; Supplemental Figure S3), suggesting that NsiR4 inhibits the initiation of translation of these two mRNAs in heterocyst-forming cyanobacteria. As shown in Figure 4, both the accumulation of the *glpX* and *pgk* mRNAs and the accumulation or activity of the corresponding enzymes are diminished in *Nostoc* strains bearing high levels of NsiR4. A secondary consequence of translation inhibition would be destabilization of the mRNAs, resulting in their degradation (Figure 4, E and F). According to a global analysis of the nitrogen-responsive transcriptome of *Nostoc*, *glpX* and *pgk* belong to a group of genes with a similar pattern of repression upon nitrogen deprivation (Brenes-Álvarez et al., 2019), suggesting the possible implication of common factors. The NtcA-regulated sRNA NsiR4 could be one such factor participating in the post-transcriptional regulation of these two genes.

Expression of NsiR4 is induced in vegetative cells upon removal of combined nitrogen (Figure 2), which is what would be expected for a gene positively regulated by NtcA. In addition, there is a stronger induction in heterocyst than in vegetative cells (Figure 2A). This complex pattern of expression is similar to that of NsiR3, another NtcA-regulated sRNA (Álvarez-Escribano et al., 2021) and could ultimately be a consequence of the higher concentration of NtcA present in heterocysts versus vegetative cells (Olmedo-Verd et al., 2006; Sandh et al., 2014). The differential accumulation of NsiR4 in heterocysts could result in differential regulation of *glpX* and *pgk* in these cells, as summarized in the proposed model (Figure 5). A quantitative proteomic study in *N. punctiforme* (Sandh et al., 2014) showed that the amount of several proteins involved in CO₂ fixation through the Calvin cycle were reduced in heterocysts and, in fact, SBPase was the protein with the lowest ratio of abundance in heterocyst versus vegetative cells. Similarly, a transcriptomic study carried out in *Anabaena variabilis* reported that the amount of *pgk* transcript was reduced in heterocysts versus vegetative cells (Park et al., 2013). In the case of SBPase, two post-transcriptional regulatory mechanisms would contribute to

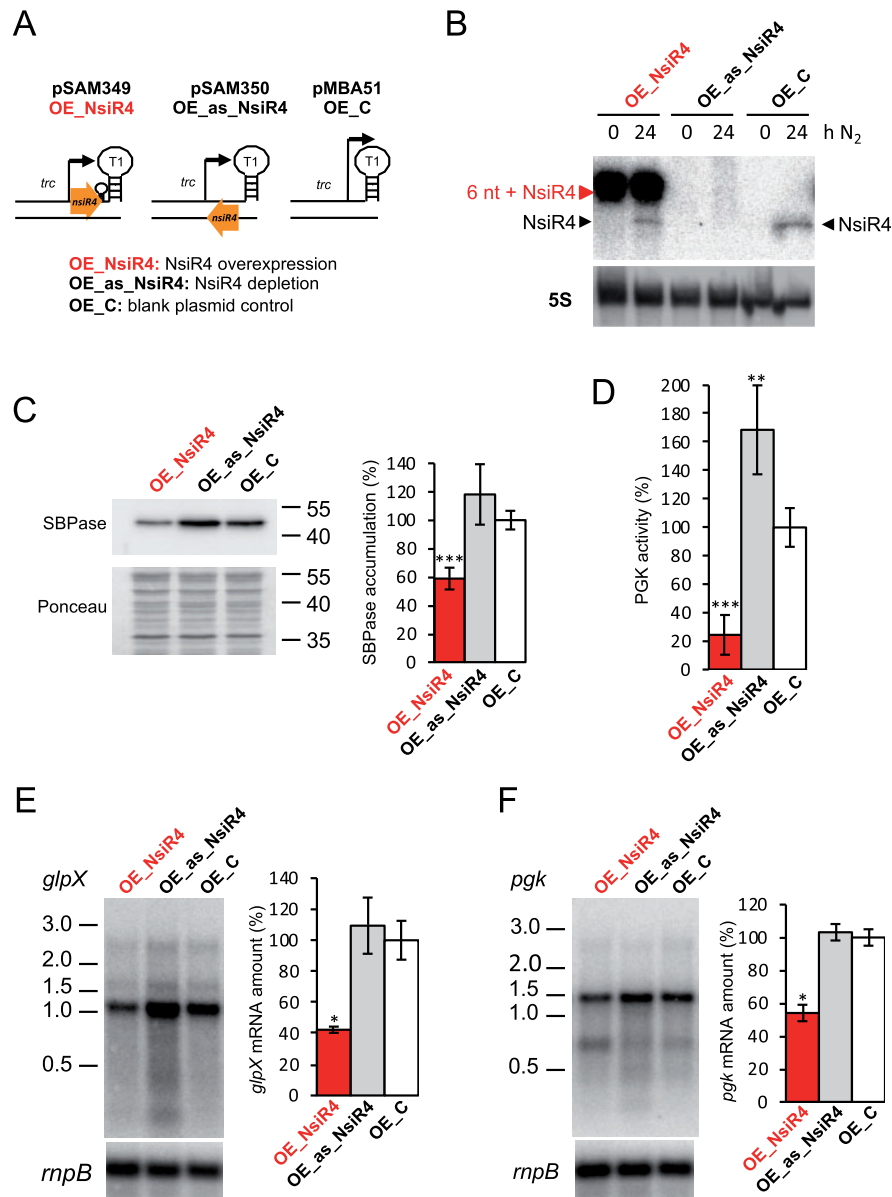


Figure 4 Effect of NsiR4 on the amount of SBPase protein, PGK activity, and the accumulation of *glpX* and *pgk* mRNAs in *Nostoc*. **A**, Scheme of the DNA fragments cloned into the plasmids used to generate the different strains with altered levels of NsiR4 (orange arrows). TSS (bent arrows), Rho-independent terminator of NsiR4 (small stem-loop), T1 terminator (large stem-loop) and the *trc* promoter are indicated. **B**, Northern blot using RNA extracted from strains OE_C, OE_NsiR4, and OE_as_NsiR4 grown in the presence of nitrate (0) or 24 h after nitrogen removal (24), hybridized with a probe for NsiR4 (top) or 5S RNA (bottom) used as loading control. Endogenous NsiR4 (black triangles) and the 6-nt-longer NsiR4 version constitutively expressed from the *trc* promoter (red triangle) are indicated. Samples contained 10 µg of total RNA. **C**, Accumulation of SBPase in strains with altered levels of NsiR4 was analyzed by Western blot in samples containing 40 µg of soluble fraction from cells grown in the presence of nitrate and transferred to medium containing no source of combined nitrogen for 24 h. Western blots were quantified with ImageLab software (Bio-Rad, Hercules, CA, USA) and normalized to Ponceau Red staining. The position of size markers (in kilodalton) is indicated on the right side. Four technical replicates of two different clones of each strain were quantified. Values are expressed as percentage of the normalized SBPase amount with respect to the amount in the control strain (OE_C), which was considered 100%. **D**, PGK activity in strains with altered levels of NsiR4 was measured in crude extracts from cells analyzed in (C). Assays were performed in duplicate with two different clones of each strain. Specific activity is expressed as percentage of the activity (2.1 U/mg protein) in the control strain (OE_C), which was considered 100%. **E** and **F**, Accumulation of *glpX* (E) or *pgk* (F) mRNAs in strains with altered levels of NsiR4 were analyzed by Northern blot in the same cells analyzed in (C and D). The position of size markers (in kilobase) is indicated on the left side. Data from two different clones of each strain were quantified and the amount of *glpX* or *pgk* mRNA was normalized to the amount of *mpB* RNA. Values are expressed as percentage of the *glpX* or *pgk* RNA amount, normalized with respect to RNA amount in the control strain (OE_C), which was considered 100%. Samples contained 3.5 µg of total RNA. **C–F**, The data are presented as the mean ± standard deviation. *T* test **P* < 0.05; ***P* < 0.01; ****P* < 0.001.

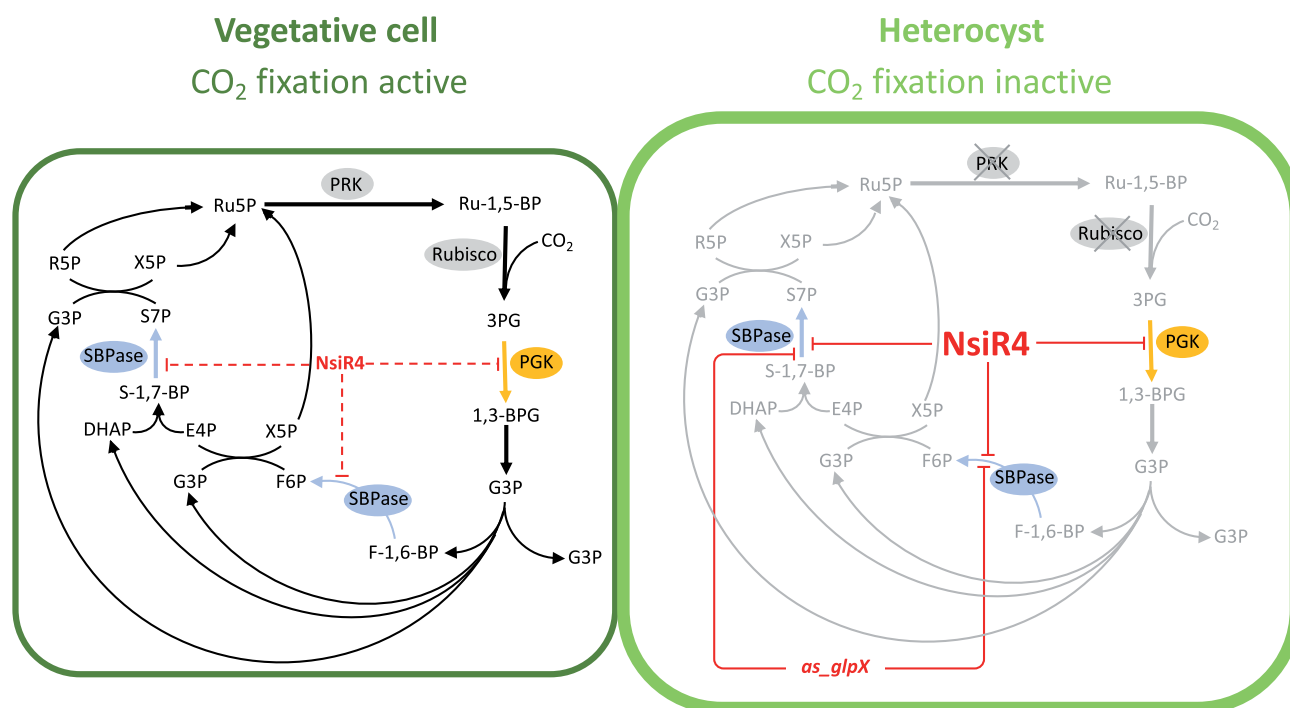


Figure 5 Schematic representation of the enzymatic reactions carried out by SBPase (in blue) and PGK (in orange) in the context of the Calvin-Benson cycle, together with the regulatory effects described here for NsiR4. The differential accumulation of NsiR4 in heterocysts versus vegetative cells is indicated with different font size and solid versus dashed red lines. Previously described regulation of SBPase by a heterocyst-specific antisense RNA (Olmedo-Verd et al., 2019) is also indicated. Gray crosses on PRK and Rubisco highlight that these enzymes are absent in heterocysts (Codd and Stewart, 1977; Codd et al., 1980; Cossar et al., 1985). 1,3-BPG, 1,3-bisphosphoglycerate; 3PG, 3-phosphoglycerate; DHAP, dihydroacetone phosphate; E4P: eritrose-4-phosphate; F-1,6-BP, fructose-1,6-bisphosphate; F6P, fructose-6-phosphate; G3P, glyceraldehyde-3-phosphate; R5P, ribose-5-phosphate; Ru-1,5-BP, ribulose-1,5-bisphosphate; Ru5P, ribulose-5-phosphate; S-1,7-BP, sedoheptulose-1,7-bisphosphate; S7P, sedoheptulose-7-phosphate; X5P, xilulose-5-phosphate. The reduced operation of CO₂ fixation in heterocysts versus vegetative cells is indicated by gray arrows.

such differential accumulation, namely, the previously described operation of a heterocyst-specific antisense RNA (*as_glpX*; Olmedo-Verd et al., 2019) and the negative regulation by NsiR4 described here. Because SBPase has been identified as a rate-limiting enzyme in the Calvin cycle in cyanobacteria and plants (Ding et al., 2016; De Porcellinis et al., 2018), reduced amounts of SBPase in heterocysts likely contribute to shutdown of CO₂ fixation in these specialized cells. In the case of PGK, speculation on the redistribution of metabolic fluxes in heterocysts versus vegetative cells may be more complex, since PGK is not only involved in the Calvin cycle but is also required for glycolysis that, in principle, is active in heterocysts. In any case, the negative regulation exerted by native amounts of NsiR4 must be subtle and perhaps required for fine-tuning PGK activity under N₂-fixing conditions.

Strains overexpressing NsiR4 from a strong constitutive promoter are not able to grow under N₂-fixing conditions. Because the amount of NsiR4 in these strains clearly exceeds that present in the WT irrespective of the nitrogen status (Figure 4B), this observation can be a consequence of excessive reduction of PGK activity or pleiotropic effects due to

interactions of NsiR4 with additional targets yet to be identified.

sRNA regulation of enzymes involved in primary carbon metabolism seems to be widespread in cyanobacteria. In *Prochlorococcus*, a cyanobacterium distantly related to *Nostoc*, several enzymes of carbon primary metabolism, including *pgk*, might be regulated by sRNAs and antisense RNAs (Lambrecht et al., 2019). Our results indicate that CO₂ fixation can be modulated by a nitrogen stress-inducible sRNA that downregulates enzymes of the Calvin cycle. Modulation of *glpX* and *pgk* in vegetative cells might also be necessary to fine-tune carbon assimilation rate to nitrogen availability while mature heterocysts become functional and under N₂-fixing conditions (Figure 5). The observed induction of expression of NsiR4 also in vegetative cells, although much weaker than that observed in heterocysts, suggests NsiR4 could be a relevant factor for adapting carbon metabolism to nitrogen deficiency.

In the unicellular strain *Synechocystis*, the NsiR4 homolog has been described to regulate the accumulation of IF7 (Klähn et al., 2015). Such a regulatory circuit constitutes a feed-forward loop, since transcription of *gifA*, encoding IF7,

is also under control of NtcA (García-Domínguez et al., 2000). In the case of *Nostoc*, the mRNA of *gjfA* is not predicted as a target of NsiR4 in the informatic screening. In fact, NsiR4 from *Nostoc* and homologs identified in heterocystous strains (Supplemental Figure S1) lack the 19 nt 5'-extension that in NsiR4 from *Synechocystis* is involved in the interaction of NsiR4 and the *gjfA* mRNA, encoding IF7 (Klähn et al., 2015). These observations suggest functional diversification of NsiR4, with different targets being modulated in different groups of cyanobacteria.

In the context of heterocyst differentiation, post-transcriptional regulation of gene expression would represent an additional level of control of the metabolic transformation of vegetative cells into heterocysts. As described above for NsiR4, the observed strong expression of other NtcA-regulated sRNAs in heterocysts could contribute to differential gene expression in these specialized cells. In this context, NsiR3, another NtcA-regulated sRNA that shows stronger expression in heterocysts than in vegetative cells, would contribute to differential regulation of proline oxidase, whose diminished levels in heterocysts could facilitate channeling of arginine to the biosynthesis of cyanophycin granules (Álvarez-Escribano et al., 2021). Mixed regulatory circuits involving transcription factors and non-coding RNAs could eventually achieve a more efficient and fine-tuned response than can be expected from purely transcriptional regulation (Nitzan et al., 2017), thus improving the fitness of microorganisms exposed to highly dynamic environments.

Materials and methods

Strains and growth conditions

Cultures of *Nostoc* WT and *hetR* derivative strain 216 were bubbled with an CO₂/air mixture (1% v/v) and grown photoautotrophically at 30°C in BG11 medium (Rippka et al., 1979) containing ferric citrate instead of ammonium ferric citrate, and lacking NaNO₃ but containing 6 mM NH₄Cl, 10 mM NaHCO₃, and 12 mM *N*-tris (hydroxymethyl) methyl-2-aminoethanesulfonic acid-NaOH buffer (pH 7.5). Nitrogen deficiency was induced by filtering, washing and resuspending cells in nitrogen-free BG11 medium containing 10 mM NaHCO₃. Growth tests (Supplemental Figure S4) were performed in nitrate-containing or nitrogen-free BG11 medium containing 10 mM NaHCO₃ (BG11C). For the culture of overexpressor strains, cells were incubated with agitation at 30°C for 1 week in flasks containing liquid BG11 medium and nitrogen deficiency was induced as described above, resuspending cells in nitrogen-free medium. Culture media was solidified with 1% (w/v) Bacto Agar (Difco, Franklin Lakes, NJ, USA). Strains used in this work are shown in Supplemental Table S1.

Nostoc strains bearing plasmids pMBA51, pSAM349, pSAM350, or pELV71 were grown in the presence of streptomycin and spectinomycin, 2 µg/mL each (liquid medium) or 3 µg/mL each (solid medium). *Escherichia coli* strains were grown in LB medium, supplemented with appropriate antibiotics (Sambrook and Russell, 2001).

Nostoc strains construction

Plasmids and oligonucleotides used in this work are described in Supplemental Tables S2 and S3. The sequences of all fragments amplified by polymerase chain reaction (PCR) were entirely verified by sequencing. We have used pMBA37 (Olmedo-Verd et al., 2019) as a backbone for overexpressing NsiR4 or an antisense to NsiR4. The sequence encoding NsiR4 or as_NsiR4 was amplified using pSAM302 as a template and oligonucleotides 919 and M13 universal or 920 and 921, respectively. The products were digested with NsiI and XhoI and cloned between the NsiI and XhoI sites in pMBA37 (between the *trc* promoter and the *T1* terminator from *E. coli rrnB* gene), rendering pSAM349 (NsiR4) and pSAM350 (as_NsiR4) (Supplemental Table S2). pMBA51, a plasmid that overexpresses a control RNA corresponding only to the *T1* terminator under the *trc* promoter (Olmedo-Verd et al., 2019), pSAM349 and pSAM350 were introduced in *Nostoc* WT by conjugation (Elhai and Wolk, 1988) generating strains OE_C, OE_NsiR4, and OE_as_NsiR4, respectively (Supplemental Table S1). The inserts in pMBA51, pSAM349, and pSAM350 are shown in Supplemental Table S4.

To generate a plasmid bearing a fusion between the promoter of NsiR4 and a promoterless *gfpmut2* gene in *Nostoc*, the promoter region (−129 to +9 with respect to the TSS of NsiR4) was amplified with primers 406 and 407 and cloned into pSpark, rendering pELV56. The ClaI-XhoI fragment containing P_{NsiR4} was cloned into ClaI-XhoI-digested pCSAM201 (Ionescu et al., 2010), rendering pELV64. The EcoRI fragment of pELV64 containing the transcriptional fusion between P_{NsiR4} and *gfpmut2* was cloned into EcoRI-digested pCSEL24 (Olmedo-Verd et al., 2006), rendering pELV71.

Reporter assay for in vivo verification of targets in *E. coli*

We used a previously described reporter assay (Urban and Vogel, 2007) and fusions to the gene *sfgfp* in plasmid pXG10-SF (Corcoran et al., 2012) for experimental target verification in *E. coli*. In this system both the GFP fusions and NsiR4 are transcribed constitutively. 5'-UTR of *glpX* and *pgk* were cloned into pXG10-SF from their corresponding TSS, according to Mitschke et al. (2011), to 60 nt within the coding region. To facilitate translation in *E. coli*, the GTG start codon of *glpX* mRNA was replaced by ATG using overlapping PCR and oligonucleotides specified in Supplemental Table S3. PCR fragments containing the region to be cloned were amplified using genomic DNA as template and oligonucleotides specified in Supplemental Table S3. Fragments were digested with NsiI and NheI and cloned into pXG10-SF treated with the same enzymes, resulting in translational fusions of the different targets to sfGFP (Supplemental Table S5).

To express NsiR4 in *E. coli*, the sequence encoding NsiR4 was amplified from genomic DNA using primers 274 (5'-phosphorylated) and 275. The PCR product was digested with XbaI and fused to a plasmid backbone that was amplified from pZE12-luc with primers PLLacOB and PLLacOD

(Urban and Vogel, 2007) and digested with XbaI, rendering pELV24 (Supplemental Table S2). For the mutagenesis of NsiR4 and the 5'-UTRs of *glpX* and *pgk*, mutations were introduced by overlapping PCR with primers containing the desired changes (Supplemental Table S3), and the fragments were cloned in the same way as the corresponding WT versions (see Figure 3).

Combinations of plasmids bearing *nsiR4* (or its mutated version) and the 5'-UTRs of target genes (or the mutated version) were introduced into *E. coli* DH5 α . Plasmid pJV300 expressing an unrelated RNA was used as a control. Fluorescence measurements were carried out with a microplate reader (VarioskanLux; Thermo Fisher Scientific, Waltham, MA, USA) using liquid cultures from eight individual colonies of cells carrying each plasmid combination, as previously described (Wright et al., 2013).

RNA isolation and Northern blot analysis

Total RNA was isolated using hot phenol as described (Mohamed and Jansson, 1989) with modifications (Brenes-Álvarez et al., 2016). Samples for Northern blot hybridization of NsiR4 were separated in 8% (w/v) urea–polyacrylamide gels as described (Steglich et al., 2008). Samples for Northern blot hybridization of longer transcripts (*glpX* or *pgk*) were treated with DNase (Turbo DNA free kit; Invitrogen, Waltham, MA, USA), separated in 1% (w/v) agarose denaturing formaldehyde gels, and transferred to Hybond-N+ membrane (GE Healthcare, Chicago, IL, USA) with 20 \times SSC buffer. Strand-specific ³²P-labeled probes were prepared with Taq DNA polymerase using a PCR fragment as template and the oligonucleotides specified in Supplemental Table S3 in a reaction with [α -³²P]dCTP and one single oligonucleotide as primer (corresponding to the complementary strand of the sRNA or mRNA to be detected). The PCR fragment for the NsiR4 probe was amplified with oligonucleotides M13 universal and M13 reverse and pSAM302 as template. Alternatively, oligonucleotide 47 was end-labeled with [γ -³²P]ATP and polynucleotide kinase and used as the probe for NsiR4 in the experiment shown in Figure 1. PCR fragments for *glpX* and *pgk* probes were amplified from genomic DNA using oligonucleotides 258 + 259 and 854 + 855, respectively. Hybridization to *rnpB* RNA (Vioque, 1992) or 5S rRNA probes was used as a loading and transfer control.

Fluorescence microscopy

Fluorescence of *Nostoc* filaments carrying plasmid pELV71 (Supplemental Table S2) growing on top of solidified ammonium-containing or nitrogen-free medium, was analyzed and quantified as described (Muro-Pastor, 2014) using a Leica HCX PLAN-APO 63 \times 1.4 NA oil immersion objective attached to a Leica TCS SP2 laser-scanning confocal microscope. Samples were excited at 488 nm by an argon ion laser and the fluorescent emission was monitored by collection across windows of 500–538 nm (GFP, shown in green) and 630–700 nm (photosynthetic pigment autofluorescence, shown in magenta). Images were analyzed with ImageJ, version 2.1.0/1.53c software (Schindelin et al., 2012).

Cell fractionation, Western blotting, and enzymatic assays

For Western blot analysis, crude extracts were prepared using glass beads. Cells from 25 mL cultures of OE_C, OE_NsiR4 and OE_as_NsiR4 subjected to 24 h of nitrogen deficiency were harvested by filtration, washed with 50 mM Tris–HCl pH 8, and resuspended in 500 μ L of resuspension buffer (50 mM Tris–HCl pH 8, 2 mM 2-mercaptoethanol) containing

EDTA-free protease inhibitor cocktail (Roche, Basel, Switzerland). The cellular suspension was mixed with glass beads (SIGMA, St Louis, MO, USA; 200 μ m) in an Eppendorf tube and subjected to seven cycles of 1 min vortexing plus 1 min of cooling on ice. Crude extract was separated from cell debris and unbroken cells by centrifugation (3 min at 3,000g at 4°C) and used for PGK activity assay. The soluble fraction obtained by centrifugation of the crude extract at 16,000g for 30 min at 4°C was used for Western blot. The protein concentration was determined by the Bradford method (Bradford, 1976) or the Lowry procedure (Markwell et al., 1978). PGK activity was determined in crude extracts by measuring NADH oxidation in a coupled assay with glyceraldehyde-3-phosphate dehydrogenase (Kuntz and Krietsch, 1982). Reaction mixtures contained 50 mM Tris–HCl pH 7.5, 1 mM MgCl₂, 0.3 mM NADH, 4 mM ATP, 1 mM DTT, 10 mM 3-phosphoglycerate, 5 U/mL glyceraldehyde-3-phosphate dehydrogenase from rabbit (SIGMA), and 0.3–0.6 μ g of crude extract. The decrease in absorbance at 366 nm was monitored at 30°C on 96-wells microtiter plates using a VarioskanLux. For Western blot, 40 μ g of protein in the soluble fraction were fractionated by electrophoresis on 10% (w/v) SDS–polyacrylamide gels. Antibodies against *Synechocystis* SBPase were used.

Computational and statistical methods

Homologs of *Nostoc* NsiR4 among cyanobacteria in the Nostocales group were identified by BLAST search (Altschul et al., 1990) at National Center for Biotechnological Information (NCBI) sequence database. CopraRNA (Wright et al., 2013, 2014) was used for the prediction of the targets of NsiR4, using the homologs in the genomes of *Nostoc* sp. PCC 7120, *Trichormus variabilis* ATCC 29413, *Calothrix* sp. PCC 6303, *Cylindrospermum stagnale* PCC 7417, *Nostoc azollae* 0708, *N. punctiforme* PCC 73102, *Nostoc* sp. PCC 7524, *Rivularia* sp. PCC 7116, and *Nostoc* sp. PCC 7107. Prediction of the interaction site between NsiR4 and the 5'-UTR of *glpX* and *pgk* in *Nostoc* and other filamentous cyanobacteria was performed using IntaRNA and a segment covering positions –100 to +100 with respect to the start codon of the corresponding mRNAs (Mann et al., 2017). Alignment of NsiR4 homologs was made using Clustal Omega (Sievers and Higgins, 2014). Secondary structure of NsiR4 was predicted with RNAalifold (Gruber et al., 2008).

The Student's *t* test was used to determine statistical significance. Number of replicates can be found in the corresponding figure legends.

Accession numbers

Sequence data and accession numbers for *nsiR4*, *glpX*, and *pgk* from Nostocales cyanobacteria are indicated in [Supplemental Data sets S1, S2, and S3](#), respectively.

Supplemental data

The following [supplemental materials](#) are available in the online version of this article.

Supplemental Figure S1. The nitrogen stress-inducible RNA 4 (NsiR4).

Supplemental Figure S2. Nitrogen-responsive expression of *glpX*, *pgk*, and NsiR4 in *Nostoc*.

Supplemental Figure S3. Conservation of the predicted interaction between NsiR4 and the *glpX* or *pgk* mRNAs in cyanobacteria.

Supplemental Figure S4. Growth of OE_NsiR4, OE_as_NsiR4 and OE_C strains in the presence or absence of combined nitrogen.

Supplemental Table S1. Strains.

Supplemental Table S2. Plasmids.

Supplemental Table S3. Oligonucleotides.

Supplemental Table S4. Sequences of inserts in plasmids used for overexpression of RNAs in *Nostoc*.

Supplemental Table S5. Sequences of inserts in plasmids used for verification of sRNA–mRNA interactions in *E. coli*.

Supplemental Data set S1. Sequences and accession numbers for *nsiR4*.

Supplemental Data set S2. Sequences and accession numbers for *glpX* (from –100 to the stop codon).

Supplemental Data set S3. Sequences and accession numbers for *pgk* (from –100 to the stop codon).

Acknowledgments

We thank Dr Francisco J. Florencio (Universidad de Sevilla) for the *Synechocystis* anti-SBPase antibody. We also acknowledge support of the publication fee by the CSIC Open Access Publication Support Initiative through its Unit of Information Resources for Research (URICI).

Funding

This work was supported by grants PID2019-105526GB-I00/AEI/10.13039/501100011033 and BFU2016-74943-C2-1-P both from Agencia Estatal de Investigación (AEI) and FEDER, UE. M.B.Á. was the recipient of a predoctoral contract from Ministerio de Educación, Cultura y Deporte, Spain (FPU2014/05123).

Conflict of interest statement. None declared.

References

- Altschul SF, Gish W, Miller W, Myers EW, Lipman DJ (1990) Basic local alignment search tool. *J Mol Biol* **215**: 403–410
- Álvarez-Escribano I, Brenes-Álvarez M, Olmedo-Verd E, Georg J, Hess WR, Vioque A, Muro-Pastor AM (2021) NsiR3, a nitrogen stress-inducible small RNA, regulates proline oxidase expression in the cyanobacterium *Nostoc* sp. PCC 7120. *FEBS J* **288**: 1614–1629
- Álvarez-Escribano I, Vioque A, Muro-Pastor AM (2018) NsrR1, a nitrogen stress-repressed sRNA, contributes to the regulation of *nblA* in *Nostoc* sp. PCC 7120. *Front Microbiol* **9**: 2267
- Bradford MM (1976) A rapid and sensitive method for the quantitation of microgram quantities of protein utilizing the principle of protein-dye binding. *Anal Biochem* **72**: 248–254
- Brenes-Álvarez M, Minguet M, Vioque A, Muro-Pastor AM (2020a) NsiR1, a small RNA with multiple copies, modulates heterocyst differentiation in the cyanobacterium *Nostoc* sp. PCC 7120. *Environ Microbiol* **22**: 3325–3338
- Brenes-Álvarez M, Mitschke J, Olmedo-Verd E, Georg J, Hess WR, Vioque A, Muro-Pastor AM (2019) Elements of the heterocyst-specific transcriptome unravelled by co-expression analysis in *Nostoc* sp. PCC 7120. *Environ Microbiol* **21**: 2544–2558
- Brenes-Álvarez M, Olmedo-Verd E, Vioque A, Muro-Pastor AM (2016) Identification of conserved and potentially regulatory small RNAs in heterocystous cyanobacteria. *Front Microbiol* **7**: 48
- Brenes-Álvarez M, Vioque A, Muro-Pastor AM (2020b) The integrity of the cell wall and its remodeling during heterocyst differentiation are regulated by phylogenetically conserved small RNA Yfr1 in *Nostoc* sp. strain PCC 7120. *mBio* **11**: e02599-19
- Buikema WJ, Haselkorn R (1991) Characterization of a gene controlling heterocyst differentiation in the cyanobacterium *Anabaena* 7120. *Genes Dev* **5**: 112
- Codd GA, Okabe K, Stewart WDP (1980) Cellular compartmentation of photosynthetic and photorespiratory enzymes in the heterocystous cyanobacterium *Anabaena cylindrica*. *Arch Microbiol* **124**: 149–154
- Codd GA, Stewart WD (1977) Ribulose-1,5-diphosphate carboxylase in heterocysts and vegetative cells of *Anabaena cylindrica*. *FEMS Microbiol Lett* **52**: 247–249
- Corcoran CP, Podkaminski D, Papenfort K, Urban JH, Hinton JC, Vogel J (2012) Superfolder GFP reporters validate diverse new mRNA targets of the classic porin regulator, MicF RNA. *Mol Microbiol* **84**: 428–445
- Cossar JD, Rowell P, Darling AJ, Murray S, Codd GA, Stewart WDP (1985) Localization of ribulose 1,5-bisphosphate carboxylase/oxygenase in the N₂-fixing cyanobacterium *Anabaena cylindrica*. *FEMS Microbiol Lett* **28**: 65–68
- De Porcellinis AJ, Norgaard H, Brey LMF, Erstad SM, Jones PR, Heazlewood JL, Sakuragi Y (2018) Overexpression of bifunctional fructose-1,6-bisphosphatase/sedoheptulose-1,7-bisphosphatase leads to enhanced photosynthesis and global reprogramming of carbon metabolism in *Synechococcus* sp. PCC 7002. *Metab Eng* **47**: 170–183
- Ding F, Wang M, Zhang S, Ai X (2016) Changes in SBPase activity influence photosynthetic capacity, growth, and tolerance to chilling stress in transgenic tomato plants. *Sci Rep* **6**: 32741
- Elhai J, Wolk CP (1988) Conjugal transfer of DNA to cyanobacteria. *Methods Enzymol* **167**: 747–754
- Elhai J, Wolk CP (1990) Developmental regulation and spatial pattern of expression of the structural genes for nitrogenase in the cyanobacterium *Anabaena*. *EMBO J* **9**: 3379–3388
- Fay P, Walsby AE (1966) Metabolic activities of isolated heterocysts of the blue-green alga *Anabaena cylindrica*. *Nature* **209**: 94–95
- Flores E, Herrero A (2010) Compartmentalized function through cell differentiation in filamentous cyanobacteria. *Nat Rev Microbiol* **8**: 39–50
- Forchhammer K, Selim KA (2020) Carbon/nitrogen homeostasis control in cyanobacteria. *FEMS Microbiol Rev* **44**: 33–53
- García-Domínguez M, Reyes JC, Florencio FJ (2000) NtcA represses transcription of *gifA* and *gifB*, genes that encode inhibitors of glutamine synthetase type I from *Synechocystis* sp. PCC 6803. *Mol Microbiol* **35**: 1192–1201
- Georg J, Dienst D, Schürgers N, Wallner T, Kopp D, Stazic D, Kuchmina E, Klähn S, Lokstein H, Hess WR, et al. (2014) The

- small regulatory RNA SyR1/PsrR1 controls photosynthetic functions in cyanobacteria. *Plant Cell* **26**: 3661–3679
- Gruber AR, Lorenz R, Bernhart SH, Neuböck R, Hofacker IL** (2008) The Vienna RNA websuite. *Nucleic Acids Res* **36**: W70–W74
- Herrero A, Flores E** (2019) Genetic responses to carbon and nitrogen availability in *Anabaena*. *Environ Microbiol* **21**: 1–17
- Herrero A, Muro-Pastor AM, Valladares A, Flores E** (2004) Cellular differentiation and the NtcA transcription factor in filamentous cyanobacteria. *FEMS Microbiol Rev* **28**: 469–487
- Herrero A, Stavans J, Flores E** (2016) The multicellular nature of filamentous heterocyst-forming cyanobacteria. *FEMS Microbiol Rev* **40**: 831–854
- Ionescu D, Voß B, Oren A, Hess WR, Muro-Pastor AM** (2010) Heterocyst-specific transcription of NsiR1, a non-coding RNA encoded in a tandem array of direct repeats in cyanobacteria. *J Mol Biol* **398**: 177–188
- Kadowaki T, Nagayama R, Georg J, Nishiyama Y, Wilde A, Hess WR, Hihara Y** (2016) A feed-forward loop consisting of the response regulator RpaB and the small RNA PsrR1 controls light acclimation of photosystem I gene expression in the cyanobacterium *Synechocystis* sp. PCC 6803. *Plant Cell Physiol* **57**: 813–823
- Klähn S, Schaal C, Georg J, Baumgartner D, Knippen G, Hagemann M, Muro-Pastor AM, Hess WR** (2015) The sRNA NsiR4 is involved in nitrogen assimilation control in cyanobacteria by targeting glutamine synthetase inactivating factor IF7. *Proc Natl Acad Sci USA* **112**: E6243–E6252
- Kuntz GW, Krietsch WK** (1982) Phosphoglycerate kinase from animal tissue. *Methods Enzymol* **90**: 103–110
- Lambrecht SJ, Kanesaki Y, Fuss J, Huettel B, Reinhardt R, Steglich C** (2019) Interplay and targetome of the two conserved cyanobacterial sRNAs Yfr1 and Yfr2 in *Prochlorococcus* MED4. *Sci Rep* **9**: 14331
- Mann M, Wright PR, Backofen R** (2017) IntaRNA 2.0: enhanced and customizable prediction of RNA-RNA interactions. *Nucleic Acids Res* **45**: W435–W439
- Markwell MA, Haas SM, Bieber LL, Tolbert NE** (1978) A modification of the Lowry procedure to simplify protein determination in membrane and lipoprotein samples. *Anal Biochem* **87**: 206–210
- Mitschke J, Vioque A, Haas F, Hess WR, Muro-Pastor AM** (2011) Dynamics of transcriptional start site selection during nitrogen stress-induced cell differentiation in *Anabaena* sp. PCC7120. *Proc Natl Acad Sci USA* **108**: 20130–20135
- Mohamed A, Jansson C** (1989) Influence of light on accumulation of photosynthesis-specific transcripts in the cyanobacterium *Synechocystis* 6803. *Plant Mol Biol* **13**: 693–700
- Muro-Pastor AM** (2014) The heterocyst-specific NsiR1 small RNA is an early marker of cell differentiation in cyanobacterial filaments. *mBio* **5**: e01079–14
- Muro-Pastor AM, Hess WR** (2012) Heterocyst differentiation: from single mutants to global approaches. *Trends Microbiol* **20**: 548–557
- Muro-Pastor AM, Hess WR** (2020) Regulatory RNA at the crossroads of carbon and nitrogen metabolism in photosynthetic cyanobacteria. *Biochim Biophys Acta Gene Regul Mech* **1863**: 194477
- Muro-Pastor MI, Cutillas-Farray A, Perez-Rodríguez L, Perez-Saavedra J, Vega-de Armas A, Paredes A, Robles-Rengel R, Florencio FJ** (2020) CfrA, a novel carbon flow regulator, adapts carbon metabolism to nitrogen deficiency in cyanobacteria. *Plant Physiol* **184**: 1792–1810
- Nitzan M, Rehani R, Margalit H** (2017) Integration of bacterial small RNAs in regulatory networks. *Annu Rev Biophys* **46**: 131–148
- Olmedo-Verd E, Brenes-Álvarez M, Vioque A, Muro-Pastor AM** (2019) A heterocyst-specific antisense RNA contributes to metabolic reprogramming in *Nostoc* sp. PCC 7120. *Plant Cell Physiol* **60**: 1646–1655
- Olmedo-Verd E, Muro-Pastor AM, Flores E, Herrero A** (2006) Localized induction of the *ntcA* regulatory gene in developing heterocysts of *Anabaena* sp. strain PCC 7120. *J Bacteriol* **188**: 6694–6699
- Orthwein T, Scholl J, Spat P, Lucius S, Koch M, Macek B, Hagemann M, Forchhammer K** (2021) The novel PII-interactor PirC identifies phosphoglycerate mutase as key control point of carbon storage metabolism in cyanobacteria. *Proc Natl Acad Sci USA* **118**: e2019988118
- Park JJ, Lechno-Yossef S, Wolk CP, Vieille C** (2013) Cell-specific gene expression in *Anabaena variabilis* grown phototrophically, mixotrophically, and heterotrophically. *BMC Genomics* **14**: 759
- Rippka R, Deruelles J, Waterbury JB, Herdman M, Stanier RY** (1979) Generic assignments, strain stories and properties of pure cultures of cyanobacteria. *J Gen Microbiol* **111**: 1–61
- Sambrook JF, Russell DW** (2001) *In Molecular Cloning: A Laboratory Manual*. Cold Spring Harbor Laboratory, Cold Spring Harbor, NY
- Sandh G, Ramstrom M, Stensjö K** (2014) Analysis of the early heterocyst Cys-proteome in the multicellular cyanobacterium *Nostoc punctiforme* reveals novel insights into the division of labor within diazotrophic filaments. *BMC Genomics* **15**: 1064
- Schindelin J, Arganda-Carreras I, Frise E, Kaynig V, Longair M, Pietzsch T, Preibisch S, Rueden C, Saalfeld S, Schmid B, et al.** (2012) Fiji: an open-source platform for biological-image analysis. *Nat Methods* **9**: 676–682
- Sievers F, Higgins DG** (2014) Clustal Omega, accurate alignment of very large numbers of sequences. *Methods Mol Biol* **1079**: 105–116
- Steglich C, Futschik ME, Lindell D, Voß B, Chisholm SW, Hess WR** (2008) The challenge of regulation in a minimal photoautotroph: non-coding RNAs in *Prochlorococcus*. *PLoS Genet* **4**: e1000173
- Urban JH, Vogel J** (2007) Translational control and target recognition by *Escherichia coli* small RNAs *in vivo*. *Nucleic Acids Res* **35**: 1018–1037
- Vázquez-Bermúdez MF, Herrero A, Flores E** (2002) 2-Oxoglutarate increases the binding affinity of the NtcA (nitrogen control) transcription factor for the *Synechococcus glnA* promoter. *FEBS Lett* **512**: 71–74
- Vioque A** (1992) Analysis of the gene encoding the RNA subunit of ribonuclease P from cyanobacteria. *Nucleic Acids Res* **20**: 6331–6337
- Wilde A, Hihara Y** (2016) Transcriptional and posttranscriptional regulation of cyanobacterial photosynthesis. *Biochim Biophys Acta* **1857**: 296–308
- Wolk CP** (1968) Movement of carbon from vegetative cells to heterocysts in *Anabaena cylindrica*. *J Bacteriol* **96**: 2138–2143
- Wright PR, Georg J, Mann M, Sorescu DA, Richter AS, Lott S, Kleinkauf R, Hess WR, Backofen R** (2014) CopraRNA and IntaRNA: predicting small RNA targets, networks and interaction domains. *Nucleic Acids Res* **42**: W119–W123
- Wright PR, Richter AS, Papenfort K, Mann M, Vogel J, Hess WR, Backofen R, Georg J** (2013) Comparative genomics boosts target prediction for bacterial small RNAs. *Proc Natl Acad Sci USA* **110**: E3487–E3496
- Zhang CC, Zhou CZ, Burnap RL, Peng L** (2018) Carbon/nitrogen metabolic balance: lessons from cyanobacteria. *Trends Plant Sci* **23**: 1116–1130